

2016

A thermo-activated wall for load reduction and supplementary cooling with free to low-cost thermal water

Yuebin Yu

University of Nebraska-Lincoln, yyu8@unl.edu

Fuxin Niu

University of Nebraska-Lincoln

Heinz-Axel Guo

Tongji University, Shanghai

Denchai Woradechjumroen

Sripatum University, Thailand

Follow this and additional works at: <http://digitalcommons.unl.edu/archengfacpub>



Part of the [Architectural Engineering Commons](#), and the [Construction Engineering Commons](#)

Yu, Yuebin; Niu, Fuxin; Guo, Heinz-Axel; and Woradechjumroen, Denchai, "A thermo-activated wall for load reduction and supplementary cooling with free to low-cost thermal water" (2016). *Architectural Engineering -- Faculty Publications*. 77.
<http://digitalcommons.unl.edu/archengfacpub/77>

This Article is brought to you for free and open access by the Architectural Engineering at DigitalCommons@University of Nebraska - Lincoln. It has been accepted for inclusion in Architectural Engineering -- Faculty Publications by an authorized administrator of DigitalCommons@University of Nebraska - Lincoln.

A thermo-activated wall for load reduction and supplementary cooling with free to low-cost thermal water

Yuebin Yu,¹ Fuxin Niu,¹ Heinz-Axel Guo,² Denchai Woradechjumroen³

¹ Durham School of Architectural Engineering and Construction, College of Engineering, University of Nebraska-Lincoln, Omaha, USA

² Sino-German College Applied Sciences of Tongji University, Shanghai, China

³ Mechanical Engineering Department, School of Engineering, Sripatum University, Thailand

Corresponding author — Y. Yu, tel 402 554-2082; email yuebin.yu@unl.edu or yuebinyu@gmail.com

Abstract

A building envelope serves as a thermal barrier and plays an important role in determining the amount of energy used to achieve a comfortable indoor environment. Conventionally, it is constructed and treated as a passive component in a building thermal energy system. In this article, a novel, mini-tube capillary-network embedded and thermal-water activated building envelope is proposed to turn the passive component into active, therefore broaden the direct utilization of low-grade thermal energy in buildings. With this proposed approach, low-grade thermal water at a medium temperature close to the ambient environment can be potentially utilized to either counterbalance the thermal load or indirectly heat and cool the space. With the revealing of the idea, effects of water temperature and flow rate on the envelope's thermal performance are investigated using a transient model. The results indicate that the thermo-activated wall can be effective in stabilizing the internal surface temperature, offsetting the heat gain, and supplying cooling energy to the space in summer. Utilization of the innovation should take the cost of total energy, energy benefit and efficiency into consideration. This article illustrates how low-grade energy can be actively used as a means for achieving net-zero energy buildings.

Keywords: Thermo-activated, Building envelope, Capillary network, Renewable energy, Low-grade energy, Energy saving

1. Introduction

The building sector is one of the biggest non-renewable energy consumers that are not utilizing much of the renewable energy available in the nation, accounting for 41% of the total energy use in the U.S. [1]. About 50% of this energy is to thermally accommodate the internal and external thermal load and condition the indoor space. A further breakdown shows that nearly half of the load is associated with the heat gain and/or loss through a building envelope [2,3]. In the meantime, majority of the energy currently used in buildings is obtained from the combustion of fossil fuel; this practice not only greatly impacts the energy security of our nation but also produces negative effects to the environment [4,5]. Researches from various aspects have been conducted to reduce the excessive consumption of non-renewable energy in buildings, including, for example, improving of the theoretical efficiency of HVAC (heating ventilation and air-conditioning) equipment [6,7] and operation efficiency of building systems [8–11], and/or expanding the portion of renewable and low-grade energy sources in buildings [3,12,13]. Theoretically, thermal operation of buildings is indeed about the use of low-grade thermal energy. If this feature is fully utilized in the

building system design and operation, a much wider horizon toward the energy and environment sustainability is open. For example, in summer, the typical indoor air temperature maintained at around 22.8 °C–26.1 °C (73 °F–79 °F) can be potentially achieved with any resources at a temperature lower than the set point. The current practice of burning fossil fuel to get electricity and then drive chillers for a thermal source at around 12 °C for cooling involves great energy quality and efficiency loss. Alternatively, developing technologies to enable low-grade energy utilization in buildings can reduce primary energy consumption, peak electrical demand and our growing dependence on non-renewable energy without necessarily lowering the desired comfort level [14,15].

It is a fact that majority of low-grade energy existing in the nature is in the form of thermal energy or can be collected with a thermal process. Examples include the solar energy, rejected heat, shallow geothermal, etc. Despite the significant amount in general, this type of renewable energy is not suitable for long-distance transfer without conversion (e.g. into electricity). In the meantime, it can be barely adopted by conventional building mechanical systems for heating and cooling. A centralized HVAC system needs a high thermal gradient to carry the energy before

Nomenclature*Abbreviations*

HVAC	heating ventilation and air-conditioning
MTC	mini-tube capillary network
PCM	phase change material
PEX	polyethylene

Symbols

a_s	solar absorptivity
c	specific heat, J/(kg·K)
d	thickness, m
h	convective heat transfer coefficient, W/(m ² ·K)
k	thermal
m	mass flow rate, kg/s
q	energy, W
t	time, s or hr
A	area, m ²
C	heat capacity, J/K
D	width of wall, m
L	length, m
N	number
Nu	Nusselt number
Pr	Prandtl number
Re	Reynolds number
Q	rate of heat transfer, W
R	thermal resistance, K/W
T	temperature, °C
V	volume, m ³
Δs	distance, m
Δx	width, m

Subscripts

a, b	sequence indicator
av	average
cap	capillary network
e	external
eq	equivalent
i	internal
j	counter
in	inlet
m	counter, motor
max	maximum
min	minimum
o	outside
out	outlet
s	solar
sa	solar-air
surr	surrounding
w	water

Greek letters

a	heat transfer coefficient, W/(m ² K)
λ	thermal conductivity, W/(m·K)
θ	temperature, °C
ω	angular frequency
φ	diameter, m
ρ	specific density, kg/m ³
ε	emissivity
σ	Stefan–Boltzmann constant

it reaches the load side. In each thermal zone, energy is distributed at several locations and then diffuses toward the load side. The space is thus maintained at a dynamic equilibrium thermal condition when the distributed energy just neutralizes the load. With the analysis we can see that, inside the space, the boundary close to the external load might be the best place for the use of low-grade energy; but this opportunity has long been overlooked.

Pipe-embedded structures with water circulating inside for heating and cooling have been recently studied. The idea is to have thermo-conditioned water convey heat or coolth into the space when it is circulated through the pipes in the floor or walls. Compared to air-based systems, this approach can work with lower temperature gradients, leading to relatively easier utilization of low-grade energy sources and consuming less energy [16–19]. For example, Stetiu [19] conducted research on energy and peak power saving potential of radiant cooling systems in commercial buildings in different U.S. climates. The results indicated that, when a radiant cooling system was employed instead of a traditional all-air system, average 30% of the energy consumption and 27% of the peak power demand could be saved. In order to acquire quicker heating, less loss of floor height and less floor load, a lightweight radiant floor heating system was developed. An experimental and numerical analysis was carried out on the effects of design parameters with a mathematic model constructed for a sample room [20]. The results showed that lightweight radiant floor heating had fine thermal stability and comfort. Besides direct heating and cooling by using thermal water in the structure, energy might be stored up with a pipe-embedded high-capacitance structure for load shifting. For example, a new style of radiant floor system using PCM (phase change material)

was proposed [21]. The results showed nearly 18% savings on the energy consumption compared to a conventional case. Water-based radiant heating and cooling systems typically use flexible cross-lined PEX (polyethylene) pipes. Selected pipe diameters are usually in the range of 20 mm–40 mm with a pipe spacing between 200 mm and 300 mm [22]. Too big size and spacing will lead to uneven surface temperature and/or decreased occupant's comfort. Among the very few studies, Mikeska and Svendsen [23] investigated small diameter pipes integrated into the inner plate of sandwich elements made of high performance concrete. It was concluded that a sufficient amount of energy can be supplied to the space for comfort and economy by means of radiant heating and cooling systems using micro-tubes.

While aforementioned water-embedded structures appear close to our idea in form, they are fundamentally different. The main focus of those studies was around utilizing the internal structure for distributing heating and cooling. Because of this, the temperature of the circulated water has a narrow range and is not close to that of natural resources [24]. Mechanical heating and cooling is generally needed to produce the thermal water. Despite the benefits over airbased systems, this practice still excludes the potential of direct and large scale utilization of natural thermal resources. A pipe-embedded system used in a building envelope has barely been investigated. Moving pipes to the space boundary brings the thermal energy closer to the load. Therefore, it can greatly relax the constraints on the temperature of thermal sources and enable the use of close-to-free renewable energy sources. A concept along this line called TB (Thermal Barrier) using U-pipes of 26 mm outer diameter was proposed for indirect heating and cooling technique driven by solar thermal radiation

[25]. Polypropylene U-pipes was constructed in external walls. Fluid flows inside a U-pipes system with a variable mass flow rate and variable supply temperature to guarantee the semi-surface temperature at 17 °C all year round in their study.

In summary, there has been very limited research on thermo-activated building walls with the use of low-grade thermal water in mini-tubes for load reduction and indirect heating and cooling. The impact of water temperature variation on the internal and external heat transfer and wall's thermodynamics has not been studied either. In this paper, we present a novel idea of using embedded capillary network and low-grade thermal water to change the dynamics of conventional walls and turn them from a passive component into an active one for conditioning the space. The thermal performance of the proposed wall is analyzed by using a thermal resistance circuit model. In the remaining of this context, we first introduce the background and motivation of this research. Then, we present the transient thermal model of the wall. After that, the effects of water temperature and mass flow rate inside the capillary network on the performance of multilayer wall are investigated. The energy performance of it compared with a conventional wall is also analyzed. The paper concludes with a brief discussion on the results and the future work.

2. Background and motivation

The building envelope is a key component of energy-efficient high performance buildings. In average, about 50% of the heating and cooling load comes directly through the building envelope. To reduce the thermal load through the building envelope from the ambient environment, the common practice is to add thermal mass and thermal resistance to the wall. The added thermal mass can increase the time lag and reduce the decrement factor, which are the two indexes of a building wall's thermal performance. The thermal resistance can reduce the impact from the temperature difference and decrease the steady-state heat transfer rate across the walls.

Ideally, the building envelope should act like our skin, which can actively balance the body temperature through actions such as regulating the openness of pores. However, the current approach with fixed capacitance and resistance does not endow the function to the envelope. A proper analog of the existing building envelope to our envisioned building enclosure is like the shell of a turtle to the skin of a mammal. There are no ways to adjust the "shell" of buildings for active tuning of the "body" temperature. Conventionally, once constructed, a building envelope becomes a casted passive mass of the building, which means it may adversely act on the building under some circumstances. For example, a heavy building envelope not just blocks out the heat load from the solar and ambient air in the day time of hot summer but also reduces the dissipation rate of the internal heat to the environment in the night.

Thermo-activation of walls with low-grade thermal water in embedded MTC (mini-tube capillary) network is based on the idea as follows: in winter, when the outdoor air is cold, thermal water available naturally with a temperature between the room air temperature and the outside air temperature can be introduced to the wall to reduce the heat loss; in summer, when the outdoor air is hot and the solar radiation intensity is high, water available naturally with a temperature between the room air temperature and the outdoor air temperature can reduce the heat gain. With conventional heating and air-conditioning approaches, water within this range of temperature is generally regarded useless unless mechanical heating and cooling is added to the water or energy conversion is utilized to lift up the grade. The idea is further illustrated with Figs. 1 and 2 for a multi-layer wall in various steady-state conditions. The temperatures inside

the multilayer wall are denoted as nodes θ_1 to θ_n . The heat gains/losses are illustrated as q and the different scenarios are marked with different patterns.

1. *Figure 1 shows the summer working condition.* Without the thermal layer of MTC and water, the representative temperature of each layer of the wall gradually increases from the room air temperature (26 °C) to the solar-air temperature (34 °C) along the polyline in black. When the MTC thermal layer is introduced in, the thermodynamics of the wall can be changed. With different water temperatures, e.g. from 29 °C to 22 °C, θ_3 of the pipe-embedded layer is dragged down to offset the heat gain through the wall. When the water temperature is lower than the room air temperature (say 22 °C), the thermal layer can also provide cooling to the space. When the water is supplied at 26 °C, a neutral condition can be achieved and the internal space is thermally isolated from and thus not affected by the ambient environment;
2. *Figure 2 is the winter working condition.* When the MTC layer is not present, the wall temperature decreases along the path from inside to outside. Room air temperature is kept at 18 °C while the outdoor is -5 °C. Huge thermal energy is needed from a centralized HVAC system to offset the heat loss. Instead, if we supply 10 °C thermal water into the MTC layer, it can improve θ_3 and reduce the heat loss from the indoor to the environment. If the water can be heated to 25 °C easily with recycled heat, which is considered still low for using in any conventional heating system, it can start to not just eliminate the heat loss to the environment, but also provide heating energy to the space. The neutral condition is achieved when the water is at the same temperature of the room air.

Depending on the cost of acquiring the low-grade thermal water, the thermo-activated wall can choose to work as a thermal barrier only or a supplementary heating and cooling source. When the system is used in mild weather or swing season, no water is needed so that the heat accumulated in the space can be quickly dissipated to the ambient environment. The flexibility brought in by the MTC thermal layer and the operation algorithms to the building envelope can enable wider and more direct use of low-grade renewable energy on-site and improve thermal comfort with more preferable surface temperature. Although radiant heating and cooling and improved thermal comfort could be the side effects of the proposed innovation, we limit ourselves to the discussion on the thermal dynamic and energy performance of the wall and the impact factors.

3. Model of the MTC embedded wall

3.1. Multilayer wall with thermal capillary network

In this study, we apply the MTC thermal layer to a conventional multilayer wall. Figure 3 shows the structure of a capillary network heat exchanger and multilayer wall with capillary network. Figure 3(a) depicts that the MTC includes a group of parallel small diameter tubes. The tubes are connected to the main inlet and outlet tubes. The size and flow direction of the MTC panels can be adjusted to suit the real applications. Fast push-in fittings allow the flexible configuration of the loop. Figure 3(b) is the photo of MTC panels of a test-building in construction for supporting this research innovation.

The MTC thermo-activated wall in this study is chosen as a 1 m × 1 m panel. The layers of the wall from the inside to the outside are plaster, concrete brick, mortar with or without MTC, and concrete brick. More details are introduced in the following sections.

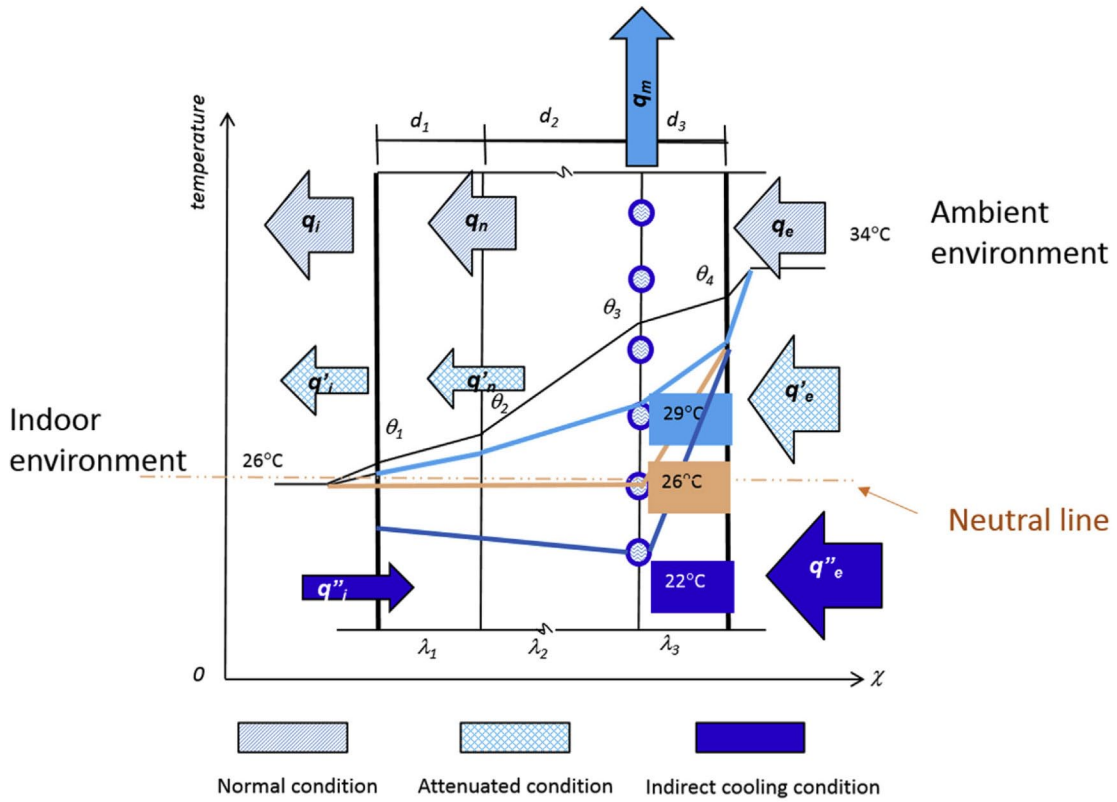


Figure 1. Illustration of steady-state temperature and thermal energy flow differences in summer.

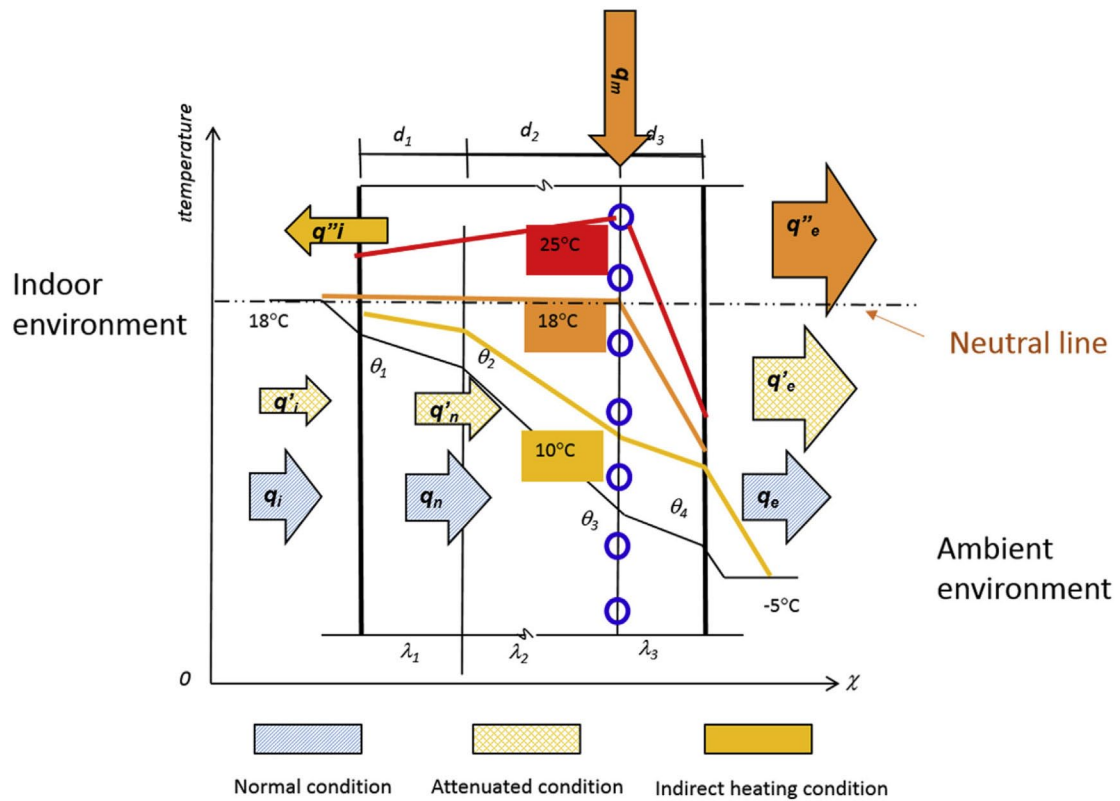


Figure 2. Illustration of steady-state temperature and thermal energy flow differences in winter.

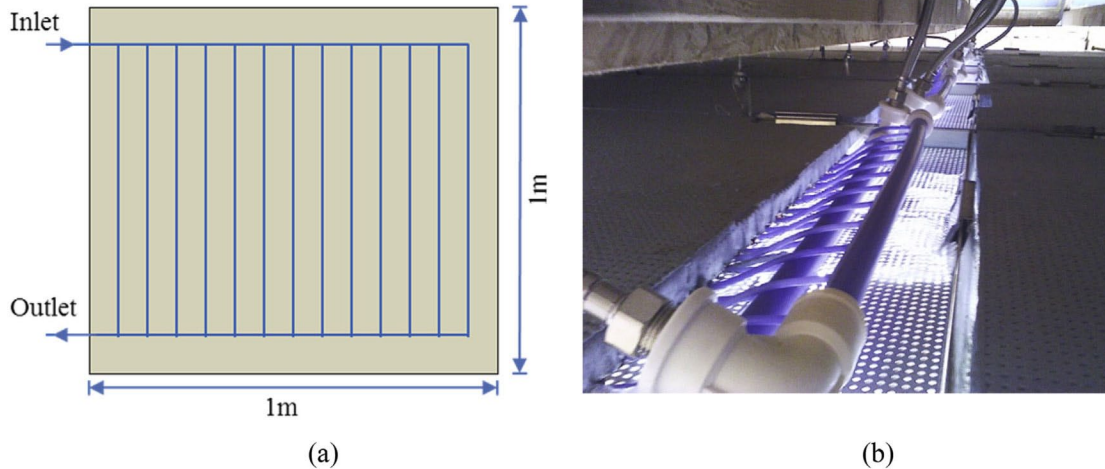


Figure 3. (a) Mini-tube capillary network; (b) The multilayer wall with capillary network.

3.2. Transient heat transfer model of the wall

Thermal capacitance and resistance network is an easy-to-use method for constructing a thermal model of buildings. The method is derived based on analogies between the thermal and electrical laws. Each layer of the wall is lumped as a node with one associated capacitance and two resistances. Consequently, node voltages and branch currents correspond to temperatures and heat flows of the layers, respectively [11]. The accuracy can be regulated by adjusting the thickness of the layers. Typically a second order ordinary equation can precisely capture the characteristics of the wall. The thermal network model is schematically shown in Figure 4. The wall model employs a one-dimensional lumped circuit that includes a finite number of distributed thermal resistances and capacitances.

Each layer j consists of one single lumped heat capacity C_j and two thermal resistances $R_{j,a}$ and $R_{j,b}$. The layer average temperature T_j is represented by the node in the middle. The number of divided layer is large enough to ensure the accuracy of assessment. Additionally, the one-dimensional simplification (transverse heat-flows negligible) is applied, which is assumed to be a rational approximation. Values of the elements in the RC-sections are determined on the basis of the thermal physical properties and geometry of the materials.

The thermal resistances of node T_j are based on Fourier's law:

$$R_{j,a} = R_{j,b} = \frac{d_j}{2 \lambda_j A} \tag{1}$$

where d_j – thickness of each layer, λ_j – thermal conductivity, and A – surface area.

The thermal capacitance is lumped as:

$$C_j = \rho \cdot c_j \cdot d_j A \tag{2}$$

where ρ – density, c_j – specific heat.

The resistances on the surfaces of the wall, Layer 1 and N , are governed by convection. The thermal resistances can be found with Newton's cooling law:

$$R_e = \frac{1}{h_e A}, \quad R_i = \frac{1}{h_i A} \tag{3}$$

where R – thermal resistance on the surface, and h – heat convection coefficient on the surface. Subscripts e and i denote the external surface and internal surface, respectively.

Temperature T_j can be obtained by applying the Kirchhoff voltage law to the node:

$$C_j \frac{dT_j}{dt} = \frac{T_{j-1} - T_j}{0.5 \cdot (R_{j-1} + R_j)} + \frac{T_{j+1} - T_j}{0.5 \cdot (R_{j+1} + R_j)} \tag{4}$$

where t is the time.

3.3. Thermal capillary network layer

The main difference between a conventional wall and the proposed MTC activated wall is the MTC thermal layer embedded in the wall. With the MTC thermal layer, there is a thermal heat source in the wall. The thermal energy transfers from the water inside the tube, through the convection and tube layer, into the motor layer. Figure 5 shows the detailed structure of capillary

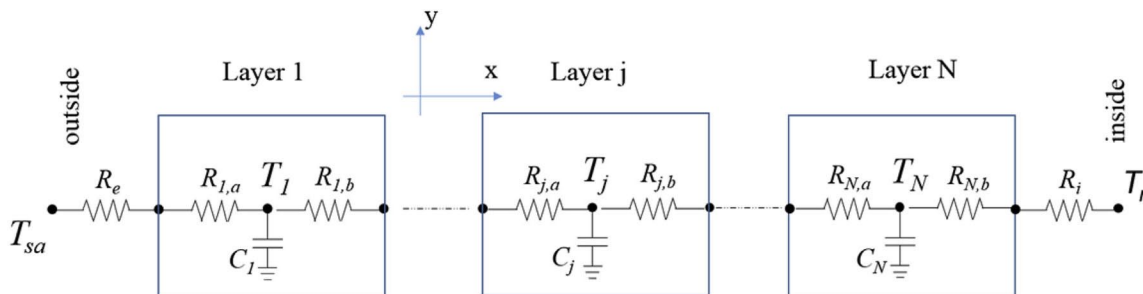


Figure 4. Thermal resistance circuit.

network filled with mortar. Due to the small volume and the high heat conductivity of mortar, the mortar temperature is considered as an even-distribution. The governing equation of the motor layer (say Layer m is the motor layer) most close to the tubes can be obtained by considering the energy balance with heat gain or loss from the water:

$$C_m \frac{dT_m}{dt} = \frac{T_{m-1} - T_m}{0.5 \cdot (R_{m-1} + R_m)} + \frac{T_{m+1} - T_m}{0.5 \cdot (R_{m+1} + R_m)} + c_w \cdot \dot{m} \cdot (T_{in} - T_{out}) \quad (5)$$

where C_m – lumped heat capacity of the motor layer m , c_w – specific heat of water, \dot{m} – water flow rate, T_{in} – supply water inlet temperature, and T_{out} – supply water outlet temperature.

The outlet water temperature of the capillary network can be computed by the lumped parameter method as follows [26, 27]:

$$T_{out} = T_m - (T_m - T_{in}) \exp\left(-\frac{\alpha_w \pi \varphi}{\dot{m} \cdot c_w} \cdot L\right) \quad (6)$$

where α_w – heat transfer coefficient from water to the tubes, φ – inner diameter of the tubes, c_w – specific heat of water, and L – length of the tube.

The flow condition in tubes is determined based on the flow condition of the inside fluid. Nusselt number is accordingly determined for the internal flow:

$$Nu = 0.023 \cdot Re^{0.8} \cdot Pr^{0.3} \quad \text{Fully developed turbulent flow} \quad (7a)$$

$$Nu = 3.66 \quad \text{Fully developed laminar flow} \quad (7b)$$

where Nu – Nusselt number, Re – Reynolds number, and Pr – Prandtl number.

The heat transfer coefficient for the internal flow can be calculated by using:

$$\alpha_w = \frac{Nu \cdot \lambda_w}{\varphi} \quad (8)$$

where λ_w – water thermal conductivity.

Meanwhile, in order to use the thermal network model defined by Equations (1)–(8), the equivalent thickness of mortar layer, d_{eq} , should be obtained:

$$d_{eq} = \frac{V_m}{A} \quad (9)$$

where $V_m = V - V_{cap}$, is the actual volume of the motor layer with the tubes removed. The two volumes, V and V_{cap} , are the volume of the motor layer and the volume taken by the tubes, respectively. They can be found by using the following equations:

$$V = x \cdot D \cdot A \quad (10)$$

$$V_{cap} = N \cdot \frac{\pi \varphi^2}{4} L \quad (11)$$

$$N = \frac{D}{\Delta s} \quad (12)$$

where D – depth of the wall, D_x – width of the motor layer, N – number of tubes in the panel, and D_s – distance between tubes.

3.4. Environmental settings

The main purpose of modeling is to investigate the thermal performance of the MTC embedded panel in terms of temperature modulation and load reduction and cooling capability when water is circulated inside. The climate is considered as having a stable pattern with about the same diurnal average over a period of several days. A sinusoidal variation is used to represent the outdoor temperature. The assumption approximates very well the exact meteorological data, and the ambient-air temperature is expressed by Reference[28]:

$$T_o(t) = T_{o,av} + \frac{|T_{o,max} - T_{o,min}|}{2} \sin\left(\omega \cdot t - \frac{\pi}{2}\right) \quad (13)$$

where T_o – outdoor air temperature. Subscripts av , max , and

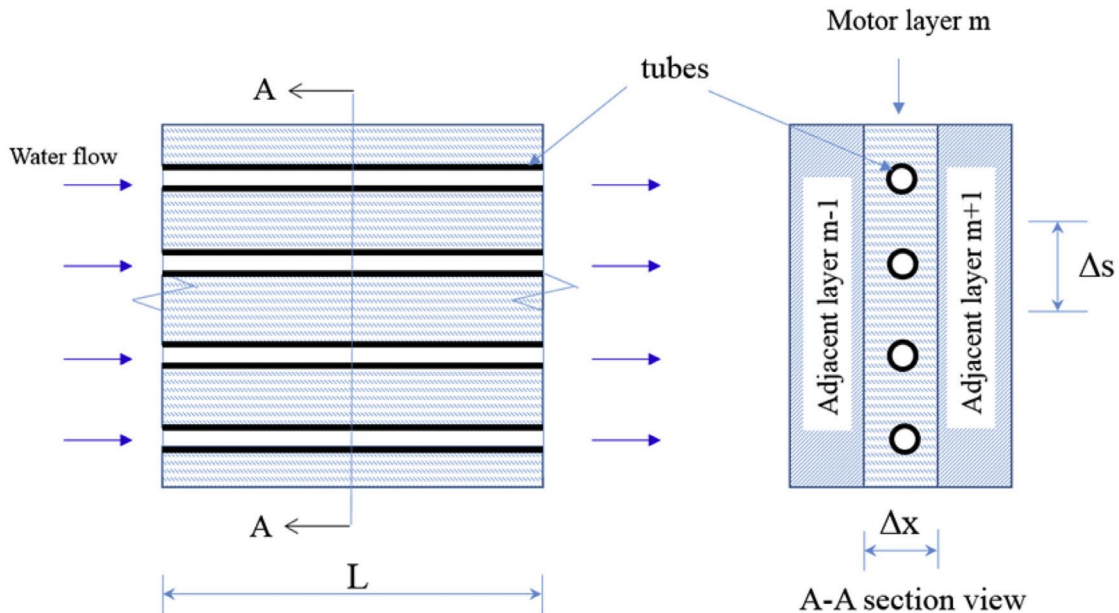


Figure 5. The detailed structure of the capillary network layer.

min denote the mean, maximum and minimum values during a day period, respectively. ω – angular frequency of the sinusoid function.

In the daytime, the solar radiation intensity greatly influences the outside surface temperature of the wall. To take the effect into account we adopt the solar-air temperature rather than the outdoor air temperature. The solar-air temperature depends on the solar absorptivity that can vary from 0 to 1. The solar-air temperature function is given by the following equation:

$$T_{sa}(t) = \left[T_o(t) + \frac{\alpha_s Q_s(t)}{h_e} \right] - \frac{\varepsilon \sigma (T_o^4 - T_{surr}^4)}{h_e} \quad (14)$$

where α_s – solar absorptivity, Q_s – solar incident radiation, h_e – heat convection coefficient on the external surface, ε – emissivity of the wall surface, σ – Stefan–Boltzmann constant, and T_{surr} – average surrounding surface and sky temperature.

The first term in Equation (14) represents the combined convection and radiation heat transfer on the surface. The last term of this equation represents the temperature correction for the radiation heat transfer when $T_{surr} \neq T_o$. It ranges from about zero for vertical wall surfaces to 4 °C for horizontal roof surfaces facing the sky due to the low effective sky temperature. As a consequence of the vertical wall, the last term is zero in the present study.

3.5. Model setting and parameters

The multilayer wall under this investigation is a 1 m by 1 m square. The MTC thermal panel is manufactured and modulated for fast installation. Tables 1 and 2 collect the thermal properties of materials and the parameters of MTC used in the simulation platform, respectively. The spaces between the tubes in the MTC layer are filled with mortar. The mini-tube of capillary network has a small diameter, 4.3 mm. The spacing of each capillary is 8 mm. Besides the design parameters and properties of the multilayer wall, the operation parameters of water inside capillary network greatly affect the performance. Table 3 shows the water temperatures and mass flow rate (velocity) options applied in the simulation. Based on the design handbook of mini-tube pipe network, four water mass flow rates (velocities) are determined. The indoor air temperature is set as 24 °C for the summer operation.

3.6. Model construction

Models of a 1 m by 1 m panel, with and without the MTC thermal layers, are constructed as 27 adjacent layers in Matlab, governed by previous equations and encapsulated as S-functions (system-functions). S-functions provide a powerful mechanism for extending the capabilities of the Simulink environment. S-functions

Table 2. Parameters of the capillary network.

	Value	unit
Diameter (φ)	4.3	mm
Spacing (Δs)	8	mm

follow a general form and can accommodate continuous, discrete and hybrid systems. S-function models for both types of walls are then placed together with the inputs and solar air calculation model in Simulink.

Figure 6 is the model with the MTC embedded thermal layer. The water temperature and flow rate are manageable inputs to the S-function. Figure 7 illustrates the model of the common brick wall without a MTC thermal layer. The platform comprises three parts: input, calculation models and output. The input part needs initial and operation conditions. For the calculation part, the structures' parameters and computing algorithm are stated and programmed. Results of the multiple layer temperature and loads can be monitored and exported by the output part. In order to eliminate the effect of initial values, a long period of four days is carried out for the performance evaluation.

4. Results analysis and performance evaluation

For MTC thermo-activated walls, besides design parameters, the water temperature and the mass flow rate are two main control variables. They are varied based on the parameters given in Table 3. Thewall without the MTC is adopted as the base case for evaluating the performance.

4.1. Solar-air temperature

In Figure 8, the solar radiation variations are given for average days with no clouds during the summer. The mean, maximum and outdoor air temperature is 26, 30, and 22 °C, respectively. The angular frequency is 0.00007269/sec. The solar radiation intensity reached the peak value of almost 500 W/m² at 1:00 pm. The solar-air temperature combined with the outdoor air temperature and solar intensity is shown in Figure 9. The solar absorptivity of the multilayer wall surface greatly affects the solarair temperature. When the absorptivity is zero, the solar-air temperature equals to the outdoor air temperature as marked with red dots (in the web version). When the absorptivity is 0.6, the peak solar-air temperature is 11 °C higher than the peak ambient air temperature. About 3.5 h time lag can be observed between the peak of solar-air temperature and air temperature as shown in Figure 9. To better understand the real situation, we adopt 0.6 for the absorptivity and the solar-air temperature marked with black squares in Figure 9 is used in the following analysis.

Table 1. Thermal properties of the wall and water.

	Thermal conductivity W/(m•°C)	Density kg/m ³	Specific heat J/(kg•°C)	Thickness m
Concrete brick	0.89	1800	1380	0.12
Mortar	0.93	1800	1050	0.01
Concrete brick	0.89	1800	1380	0.12
Plaster	0.3	800	920	0.01
Other thermal properties:	h_e : 23 W/m ² K, h_i : 8 W/m ² K Pr : 7, k : 0.6 W/m K, c_w : 4200 J/kg K			

Table 3. Operation parameters of water in the capillary network.

Parameters	Options for summer
Water temperature (°C)	24, 22, 20, 18
Water mass flow rate (velocity) kg/s (m/s)	0.00075 (0.05), 0.0015 (0.1), 0.00225 (0.15), 0.003 (0.2)

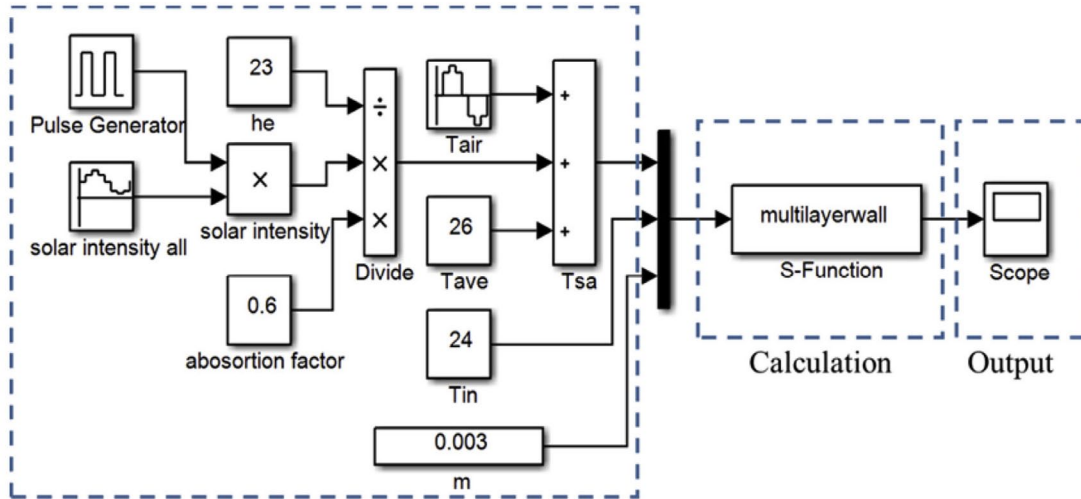
4.2. Temperature comparison with different supply water temperature

Before we apply water to the MTC thermal layer to activate the wall, we simulate the conventional wall without the capillary network. Figure 10 shows the temperatures at different layers in the conventional wall without MTC. The indoor air temperature is kept constant at 24 °C. It can be seen from the figure that the amplitude of the wall temperature fluctuation quickly reduces from the external layer (Layer 1) to internal layer (Layer 25). The external wall layer temperature, which can be considered as the external wall surface temperature due to the small thickness of divided computing element, is nearly synchronous to the solar-air temperature. The highest temperature of the external

wall surface can reach up to 36.5 °C. The internal wall surface temperature (Layer 25) has a lower fluctuation in the range of 25–27 °C. Because of the large energy storage ability the peak value time difference between the external and internal surface wall temperature is close to 10 h.

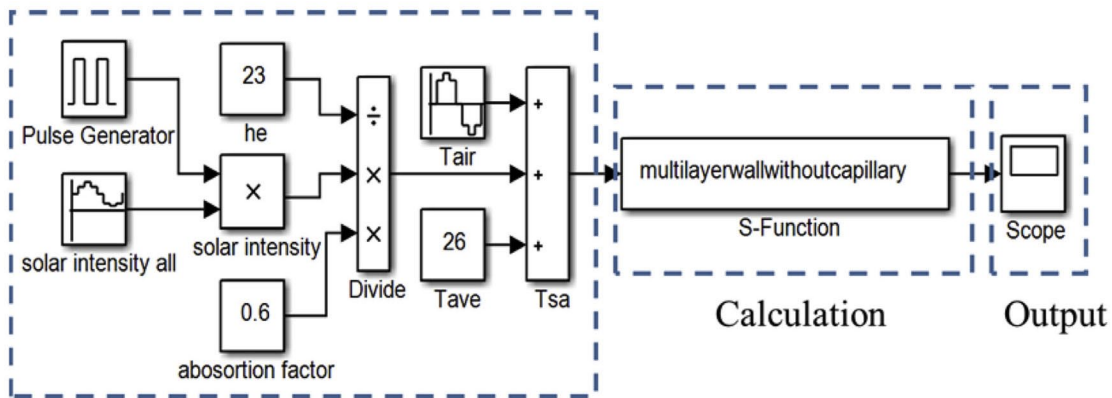
The fluctuation of the inner surface and the time lag of peak value from the external surface to the internal surface are the two important indexes to evaluate the thermodynamics of a wall. Low fluctuation means low decrement factor and good capability of the wall at attenuating the impact from the outside temperature. A stable indoor temperature is an aspect of thermal comfort. A large time lag means the wall has a high thermal capacitance to reduce the peak load from the outside. The fluctuation on the inner surface temperature may also cause decreased occupant’s thermal comfort.

Then, we supply water at different temperatures to the MTC layer to activate the wall. For this analysis, the water flow rate is set as 0.00225 kg/s with a velocity at 0.15 m/s in tubes. Figure 11 depicts the temperature of the mortar layer under different inlet water temperature conditions. As seen from the figure that the mortar temperatures are very close to the water temperature at the inlet of the capillary network due to the high heat transfer conductivity of mortar for all four conditions ($T_{in} = 24,$



Input: initial; operation condition.

Figure 6. Calculation platform of multilayer wall with capillary network.



Input: initial; operation condition.

Figure 7. Calculation platform of multilayer wall without capillary network.

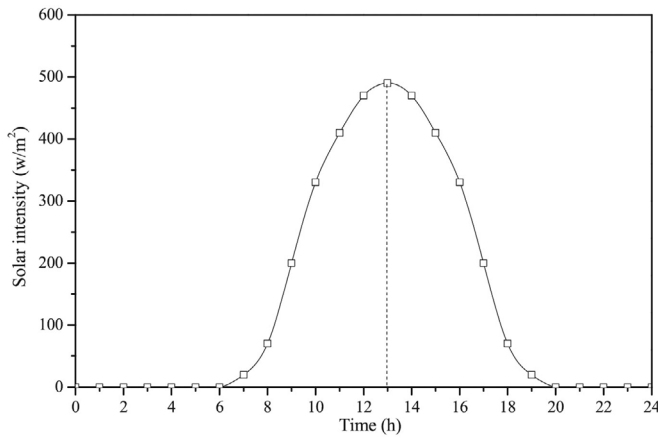


Figure 8. Solar intensity.

22, 20, and 18 °C). There is just a little fluctuation affected by the periodic change of the outdoor air temperature and solar radiation. The response is significantly different from the conventional wall. Because of the added thermal layer, the dynamics of the wall has been changed. The power of thermal water source starts to dominate. When the temperature of the motor layer is kept constant, the indoor space can be isolated from the impact of ambient environment. The original two indexes, including the time lag and decrement factor, are no longer that obviously influential to the simulated wall.

With different supply water temperatures, the internal wall surface temperature could be different and directly lead to change of the indoor cooling demand and the thermal comfort. The internal wall surface temperatures under different inlet water temperature conditions are presented in Figure 12. It can be seen from the figure that the internal wall surface temperature is equal to the indoor air temperature when the water

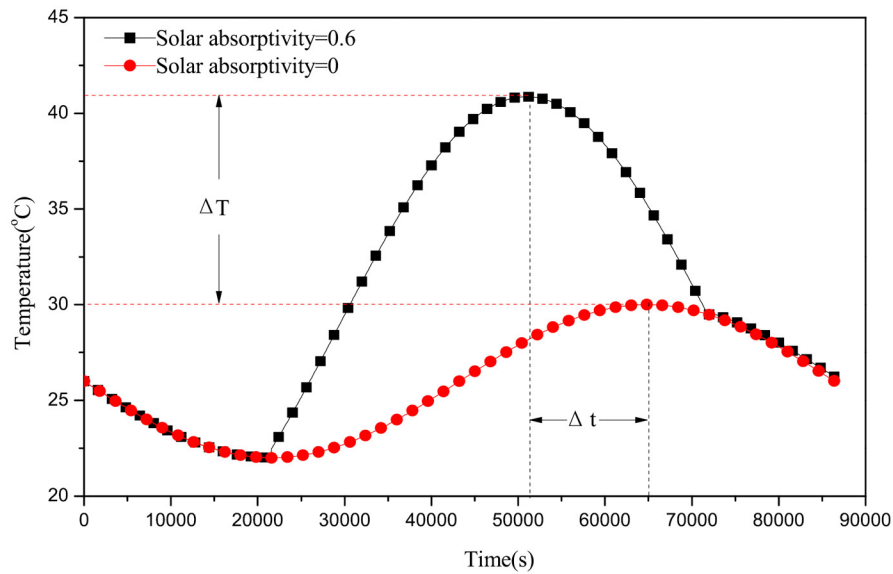


Figure 9. The solar-air temperature.

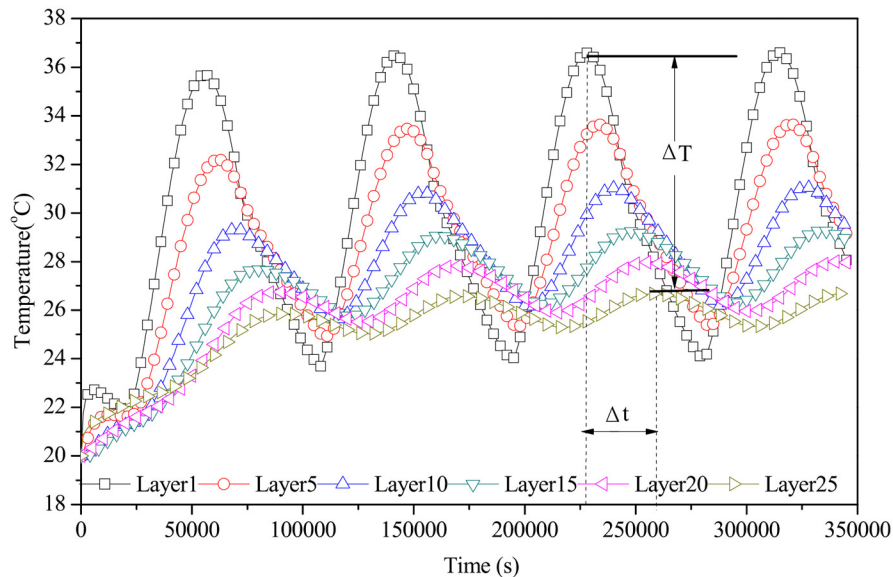


Figure 10. Temperatures of multilayer wall without MTC.

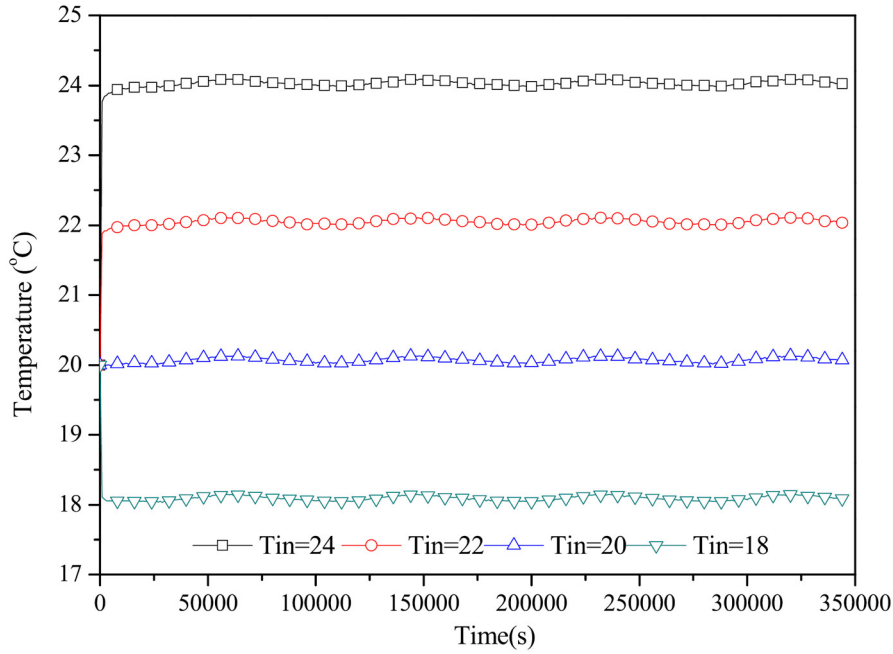


Figure 11. Mortar layer temperatures under different inlet water temperatures conditions.

temperature at the inlet of the capillary network is set the same value as the indoor air temperature at 24 °C. In other words, the wall is thermally neutralized and there is almost no cooling load generated from the wall in this condition. When the water temperature at the inlet of the capillary network is reduced to 22 °C, the internal wall surface temperature is dragged to close to 23 °C. Reducing the supply water temperature will lead to lower internal wall surface temperatures correspondingly. When the water temperature at the inlet of capillary network is set at 18 °C, the internal wall surface temperature is a little bit above 21.2 °C. The results indicate that when the water temperature at the inlet capillary is set lower than the indoor air temperature, the

wall can supply additional energy for space cooling besides counteracting the cooling load from the wall.

In order to clearly analyze the influence of inlet water temperatures on the performance, the peak values of internal wall surface temperatures under different water temperature conditions are presented in Table 4 and Figure 13. The inlet water mass flow rate of 0.00225 kg/s is selected as the operation condition. When the water temperatures are 24, 22, 20 and 18 °C, the peak value of internal wall surface temperatures are 24.06, 23.11, 22.17 and 21.22 °C, respectively. It can be seen from Figure 13 that the effect of the water temperature on the inner surface temperature is very close to linear. Based on this principle, the performance of

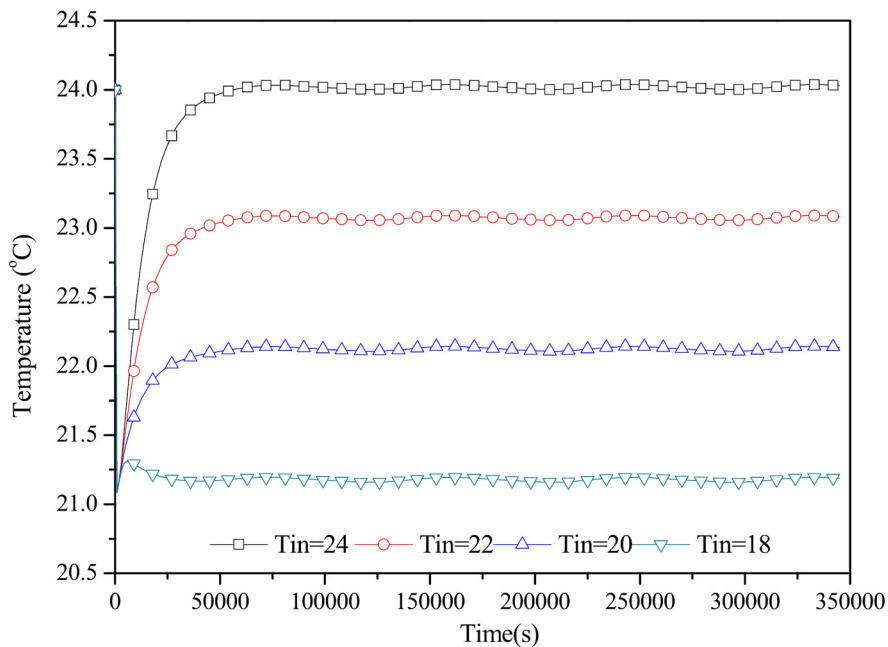


Figure 12. Internal wall surface temperatures under different inlet water temperature conditions.

internal wall surface temperature under other conditions with different inlet water temperatures can be deduced.

The water temperature at the outlet of the capillary network and the temperature difference between the inlet and outlet are shown in Figs. 14 and 15, respectively. Figure 14 indicates that the water temperature at the outlet of capillary network fluctuates just a little higher than that of the inlet side. However, as revealed in Figure 15 the water temperature difference between the inlet and outlet of the capillary network under the condition of low inlet temperature is bigger than that of the high inlet temperature condition. This tells that more energy will be released by wall surfaces to the ambient due to the lower wall surface temperatures when a low inlet water temperature is applied to the capillary network. In a real application, whether a low temperature of water should be supplied or not should be jointly determined by the cost of obtaining the water source at the temperature and the energy distribution between the inner surface and the outer surface.

4.3. Temperature comparison with different water flow rates

Besides the water temperature at the inlet of the capillary, the water flow rate might also impact the thermal performance of the MTC thermally activated wall. Based on the flow velocity design specification of pipe network for cooling and heating, four water mass flow rates of 0.00075, 0.0015, 0.00225 and 0.003 kg/s are selected as given in Table 3. For this analysis, the water temperature at the inlet of capillary network is picked as 24 °C. Figure 16 shows the external wall surface temperature under the four different conditions of mass flow rates. The results indicate almost no difference among the external wall surface temperatures. However, the internal wall surface temperatures under four different conditions are different as shown in Figure 17. The internal surface wall temperature under the condition of low flow rate is higher than the condition of high mass flow rate. A low flow rate as to 0.00075 kg/s reduces the capability of the MTC to fully eliminate the impact on the indoor space from the outdoor environment.

The peak value of internal wall surface temperatures under different water temperature conditions are presented in Table 5 and Figure 18. When the water mass flow rates are selected as 0.00075, 0.0015, 0.00225 and 0.003 kg/s and at 24 °C, the peak value of internal wall surface temperatures differs a little bit from 24.097 to 24.052 °C. It can be seen from Figure 18 that when the water mass flow rate increases, the peak value of internal wall surface temperature reduces and tends to a horizontal line at last. It means, when the water mass flow rate reaches a certain value, there will be no great influence on the performance with the wall fully being neutralized from the ambient environment. On the contrary, a much higher water flow rate might not be desirable since it can increase the energy consumption on water circulation.

4.4. Energy analysis of the MTC embedded wall

As indicated in Section 2, the application of MTC thermal layer will change the dynamics of a wall. When a wall is thermoactivated, the energy contained in the water might flow to both the internal space and the outdoor environment. When the amount of energy flows to the external surface to offset the load from the

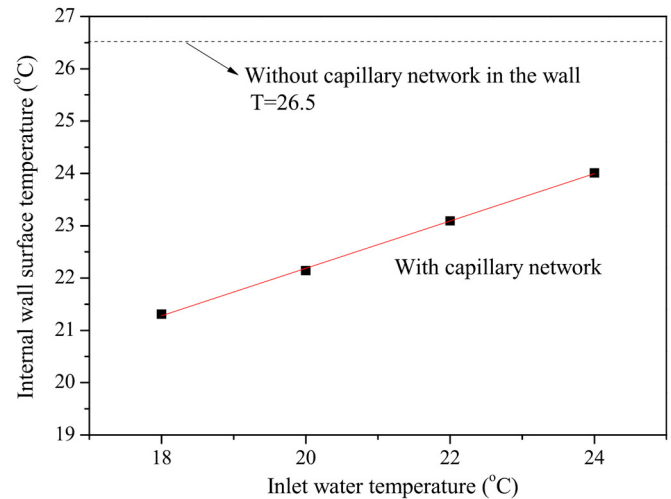


Figure 13. Internal wall surface temperature under different water temperatures.

MTC layer is much more than enough, it becomes undesirable. In this section, we focus more on the energy analysis.

Firstly, the energy performance of the multilayer wall without a capillary network is analyzed as the baseline. Figure 19 shows the cooling load generated from the 1 m² conventional multilayer wall without a capillary network. It can be seen that the cooling load fluctuates when the ambient environment changes. The peak value of the cooling load can reach to 21.5 W/m² and minimum value of the cooling load is about 10 W/m².

Figure 20 presents the power from the internal wall surface to the indoor air under the four different water temperatures of 24, 22, 20 and 18 °C. The water mass flow rate inside the capillary network is set at 0.00225 kg/s. When the water temperature at the inlet of the capillary network is 24 °C, the heat transfer between the internal wall surface and the indoor air is almost 0 W/m². In other words, the multilayer wall is totally insulated after embedding the MTC. When the water temperature at the inlet is 22 °C, the heat transfer between internal wall surface and indoor air is about -7.5 W/m². The multilayer wall not only counterbalances the cooling load through the wall but also supplies additional energy for space cooling. Compared with the condition of the water temperature at 22 °C, the heat transfer between the internal wall surface and the indoor air is much bigger under the conditions of the water temperature at 20 °C and 18 °C, which provides cooling -15 and -22.5 W/m², respectively. The results suggest that, when the water temperature at the inlet of the capillary network is lower than the indoor air temperature, the thermal water can supply cooling energy to the space in addition to the load isolation.

Figure 21 shows the impact of water mass flow rate on the heat transfer between the internal wall surface and the indoor air. The water temperature at the inlet of the capillary network is set at 24 °C. As seen from the figure, the water mass flow rate has relatively lower effect on the heat transfer. All conditions greatly reduce the thermal load from the wall. The remaining cooling load from the wall changes in the range of 0–0.8 W/m, which is almost negligible compared to that of the conventional wall.

Table 4. Peak value of internal wall surface temperature with different inlet water temperatures.

	Without capillary	With capillary Tin = 24	With capillary Tin = 22	With capillary Tin = 20	With capillary Tin = 18
Peak value (°C)	26.5	24.04	23.09	22.14	21.31

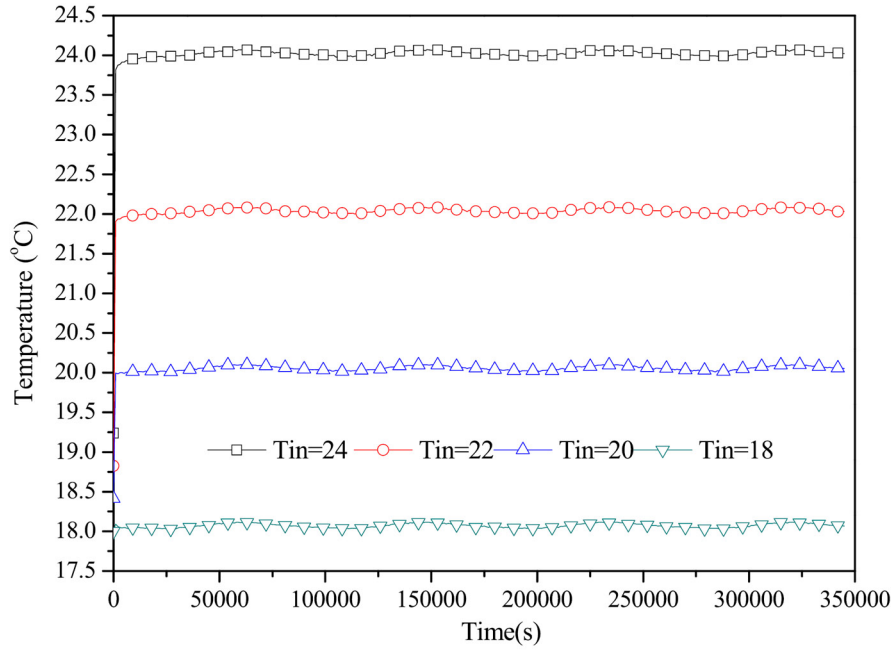


Figure 14. Water temperatures at the outlet of the capillary network.

Table 6 gives a summarized energy performance with and without the thermal MTC layer in terms of the load and cooling power. The peak cooling load reaches 21.5 W when the MTC is not applied in the wall. After application of the MTC, the cooling load varies with the change of inlet water temperature from 0.23 W to -22.4 W. The cooling load reduces greatly when the water is set at the neutral temperature (24 °C for this case), but it does not vary very much when the water mass flow rate changes from 0.00075 kg/s to 0.003 kg/s.

Based on the above energy analysis, we can see that the MTC thermo-activated wall not only can counterbalance the cooling load, but also can supply energy for space cooling when the water

at the inlet of the MTC is lower than the indoor air temperature. Water used in the capillary is of low-grade energy in summer compared with the chilled water in conventional air conditioning systems (e.g. 12 °C). The water energy difference between the inlet and the outlet of the capillary network shows the overall energy consumption to realize the building wall energy savings. It can be seen from Figure 22 that the energy difference between the inlet and the outlet of the capillary network under the condition of $T_{in} = 24$ °C reaches the peak value 80 W to counterbalance the cooling load of the wall. The peak energy difference between the inlet and the outlet of the capillary network under the conditions of $T_{in} = 22, 20$ and 18 °C are 97, 120 and 140 W,

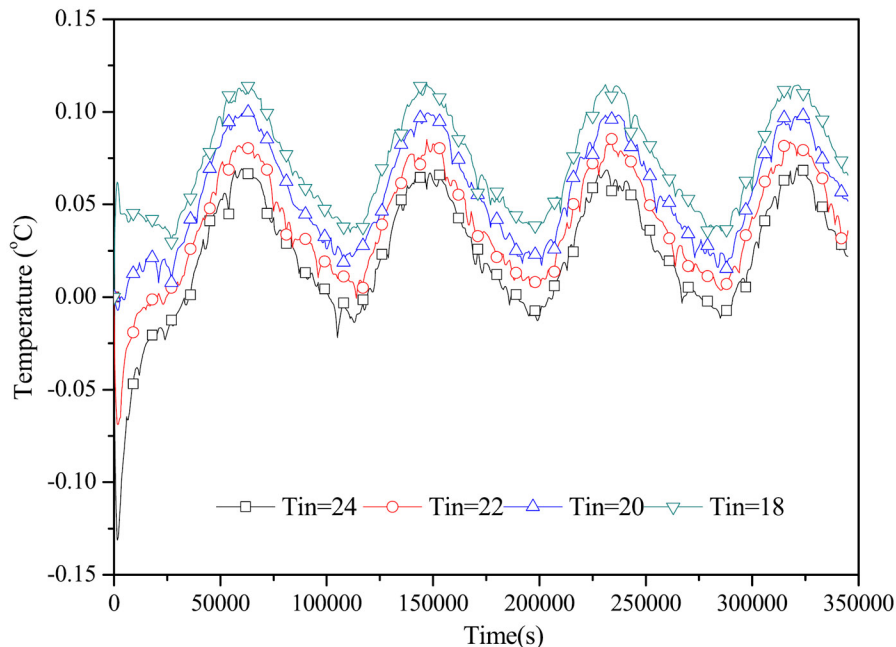


Figure 15. Water temperatures differences between the outlet and the inlet of the capillary network.

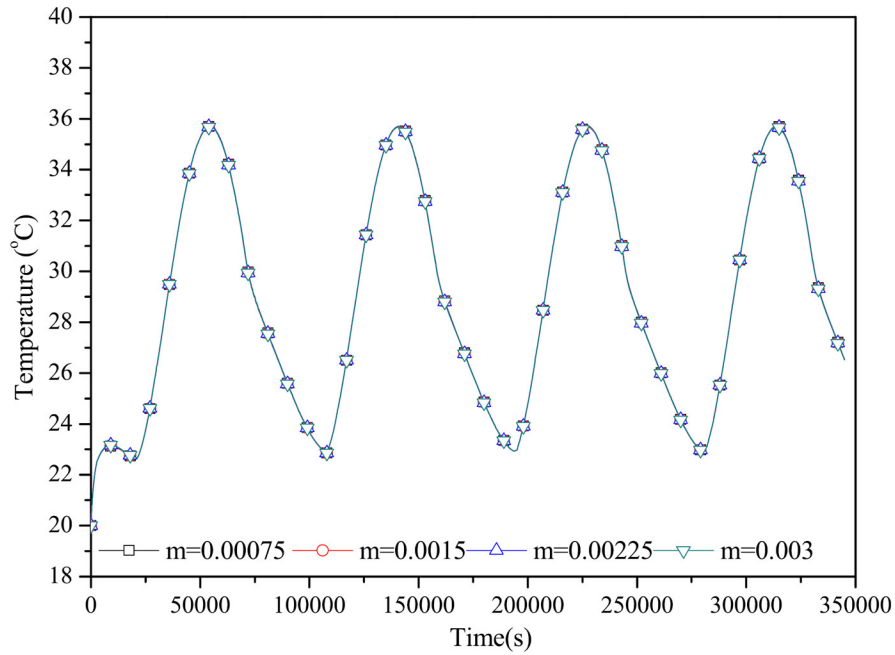


Figure 16. External wall surface temperatures with different mass flow rates.

Table 5. Peak value of internal wall surface temperature with different water mass flow rates.

	With capillary m = 0.00075	With capillary m = 0.0015	With capillary m = 0.00225	With capillary m = 0.003
Peak value (°C)	24.100	24.053	24.037	24.029

respectively. This is because that, although the wall can supply more energy for space cooling with low water temperature, it may also lead to a lower temperature on the external wall surface resulting in more energy loss. Therefore, there will be a tradeoff

relationship between the water temperature and energy benefit by utilizing the low-grade energy.

We define the energy benefit of the thermo-activated wall as the reduction of thermal load entering the space by applying the MTC against the base case without the MTC. The comparison of average energy consumption and energy benefit of various supply water temperature from the thermo-activated wall is further collected in Table 7. The water flow rate is set as 0.00225 kg/s. From the simulated values, we can tell the energy consumption grows with the energy benefit when the supply water temperature decreases. 15W is beneficial to right offset the average external load from the envelope. The overall efficiency is around

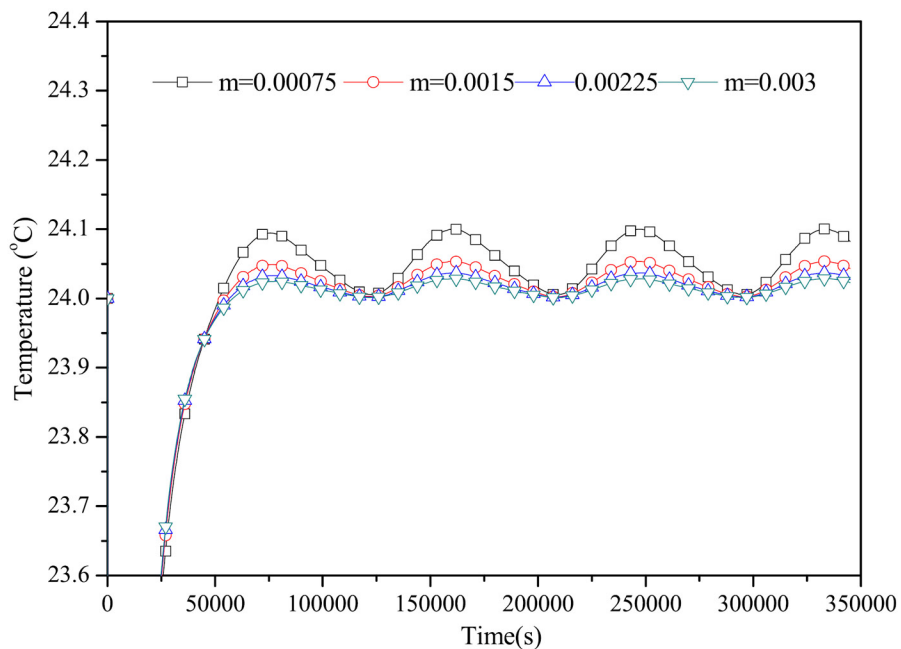


Figure 17. Internal surface wall temperatures with different mass flow rates.

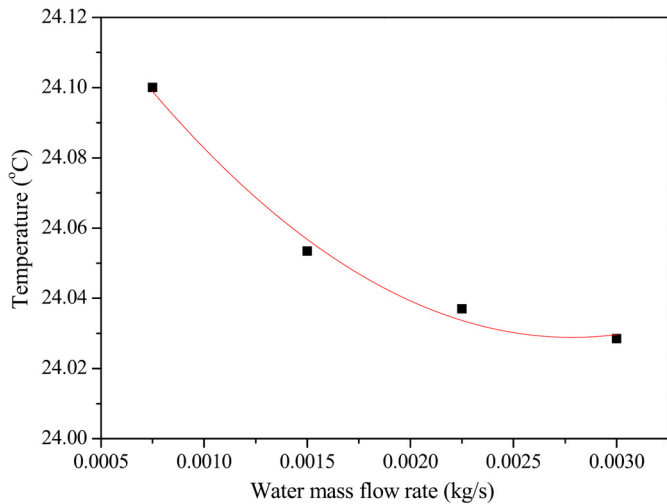


Figure 18. Internal wall surface temperature under different water mass flow rates.

42% for the simulated wall with given weather conditions. It starts to decrease slightly when the temperature is lower to 18 °C. Whether and how a lower supply water temperature should be utilized in the real applications should be jointly weighted based on the cost of obtaining the water, the energy benefit to the space and the utilization efficiency.

5. Conclusions

In this article, we proposed a novel idea of using MTC (minitube capillary) network with low-grade thermal water to thermoactivate conventional walls. Unlike a general water-embedded internal structure, our innovation applies the MTC at the boundary between the space and external environment and brings the thermal energy closer to the load. It can significantly relax the constraints on water temperature and facilitate the direct use of low-grade renewable energy in buildings without conversion, which generally is useless in industry and transportation. Water needed for the MTC thermal layer at the referred temperatures in this innovation can usually be obtained at low or no cost.

In addition to the load mitigation, the system might also supplement cooling or heating energy to the space when the temperature of circulated water suits.

To investigate the thermal dynamic performance of the wall, we established a transient dynamic model for the cases with and without the MTC thermal layer. The supply water temperature and flow rate were varied in reasonable ranges. The analysis for summer operation, including the comparison of the internal wall surface temperature, external surface temperature, energy flow, etc., was conducted. The simulated results indicated that the MTC embedded wall can greatly change the thermodynamics of the wall, from counterbalancing the impact from the ambient environment to indirectly cooling the space. The temperature and energy flow profile of the MTC thermo-activated wall were graphically illustrated.

More specifically, we conclude that:

- There was barely any cooling load coming from the wall when the water temperature at the inlet of MTC is set as the indoor air temperature.
- The thermal water layer dominates the thermal performance and greatly changes the thermodynamics of the wall. The inner surface of the wall sees almost no impact from the variation of the exterior environment in the studied cases.
- The effect of water temperature on the internal wall surface temperature is linear. Within the selected range, change on the water flow rate has little effect on the heat transfer compared to that of the water temperature.
- Energy consumption and energy benefit grow together with the decrease of water temperature applied in the capillary network.

As an active low-grade energy utilization technology, MTC thermo-activation wall potentially has less operational constraints from the architecture features and climate conditions and can be widely utilized. Investigation on the performance of MTC thermoactivated wall supplies the foundation for the optimal design and operation of building wall and zero-energy buildings in future. In the meantime, it also provides some insights on using the approach for micro-environment control. Energy use should be allocated not just based on quantity but also based on quality to better support a sustainable development of the society. Future study with real measurements is needed to further

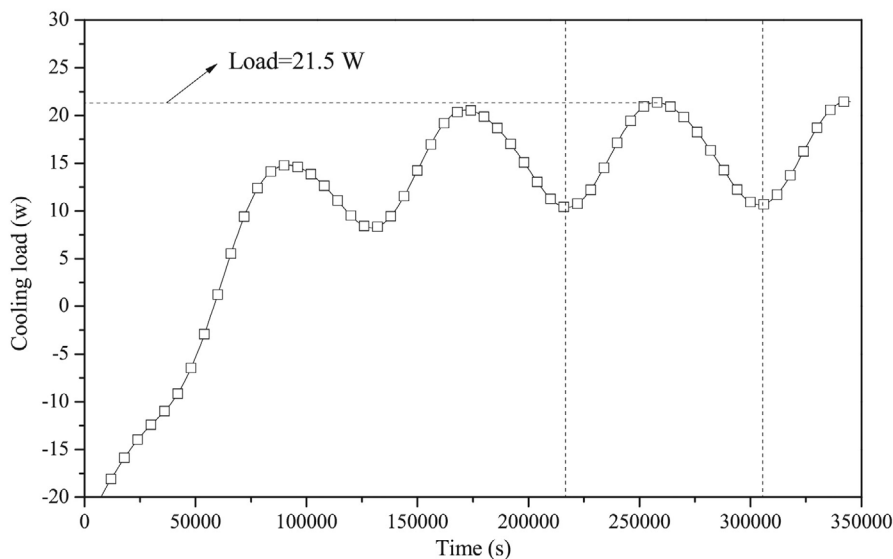


Figure 19. Cooling load generated by the conventional wall without capillary network.

Table 6. Energy performance comparison with and without capillary network.

	Without capillary	With capillary $m = 0.00225 \text{ kg/s } (^{\circ}\text{C})$				With capillary $T = 24 ^{\circ}\text{C } (\text{kg/s})$			
		$T_{in} = 24$	$T_{in} = 22$	$T_{in} = 20$	$T_{in} = 18$	$m = 0.00075$	$m = 0.0015$	$m = 0.00225$	$m = 0.003$
Load (W)	21.5	0.23	-7.3	-14.7	-22.4	0.40	0.27	0.23	0.21

Negative value means wall surface can supply cooling energy.

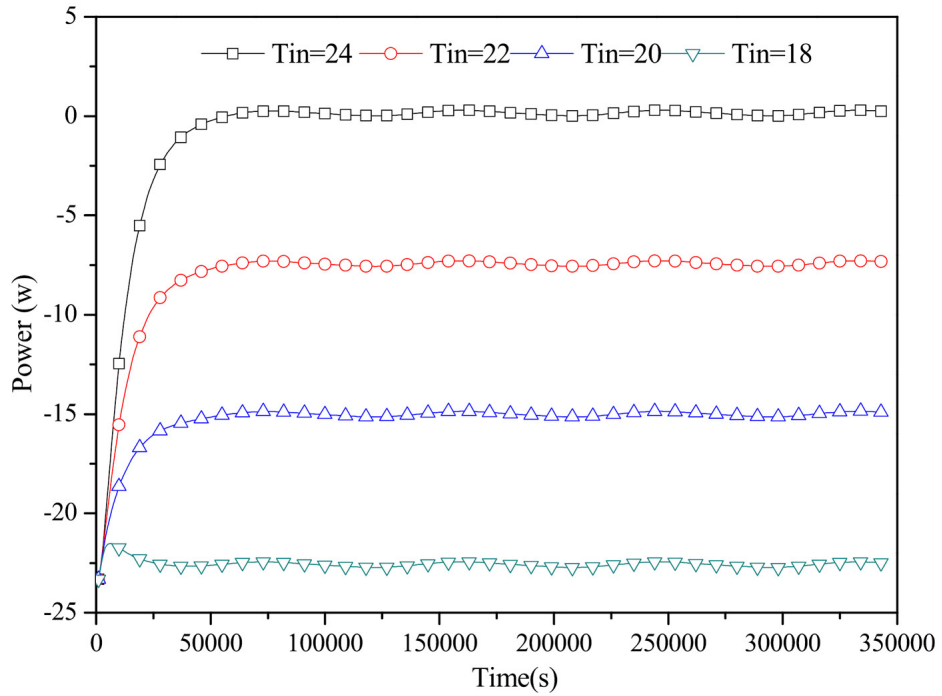


Figure 20. Cooling power with $m = 0.00225 \text{ kg/s}$ under different water temperatures.

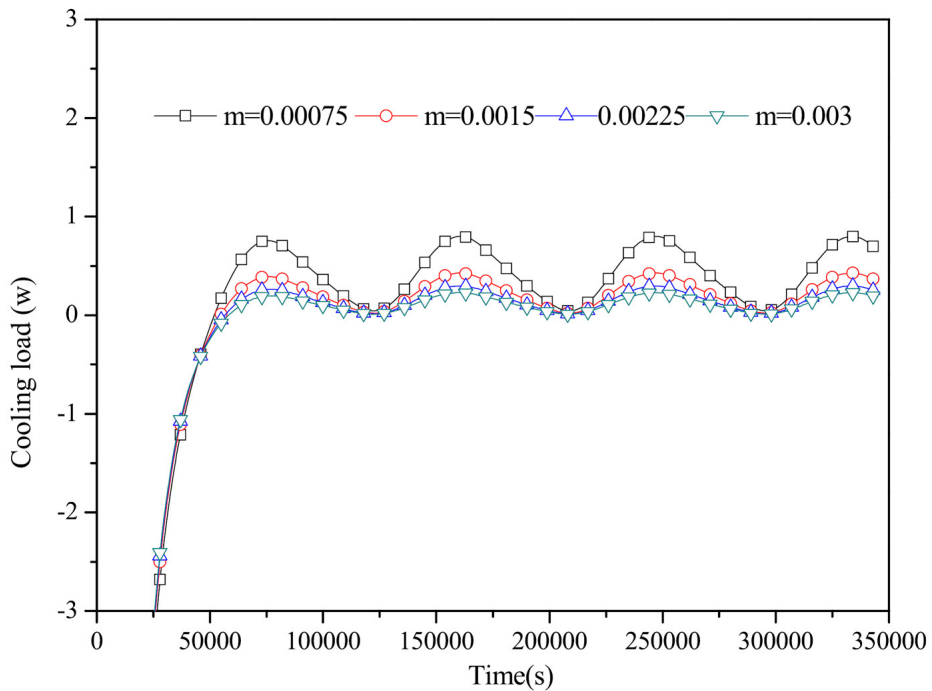


Figure 21. Cooling load with $T_{in} = 24 ^{\circ}\text{C}$ under different water mass flow rates.

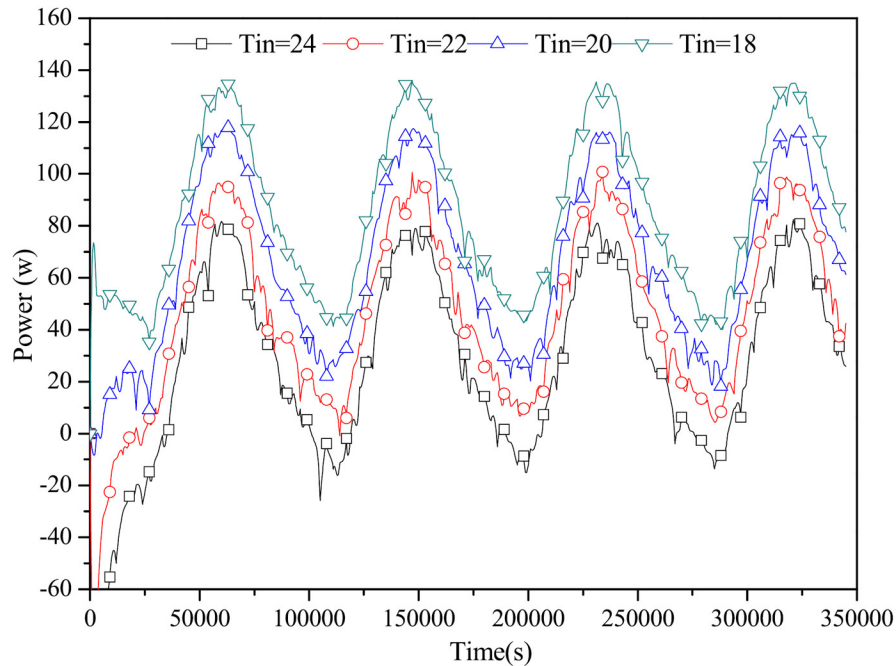


Figure 22. Energy differences between inlet and outlet of capillary network.

Table 7. Energy benefit and consumption comparison.

	Energy consumption (W)	Energy benefit (W)	Efficiency
Tin = 24	35	15	0.42
Tin = 22	53	22.5	0.42
Tin = 20	71	30	0.42
Tin = 18	91	37	0.41

explore the characteristics and value of this system with the total energy cost, indirect heating/cooling capability, energy efficiency, as well as installation considerations, included.

Acknowledgments — The authors gratefully acknowledge the support of this study from University of Nebraska-Lincoln Faculty Start-up Fund and Layman Award.

References

- Energy Information Administration (EIA). Annual energy review. 2012.
- Baderia N, Khandelwal A. Cool down – cost effectiveness in HVAC by building envelope optimization. *Buildotech Magazine*; 2011.
- Sozer H. Improving energy efficiency through the design of the building envelope. *Build Environ* 2010;45(12):2581–93.
- Energy Information Administration. Buildings energy data book. 2011.
- United Nations Environment Programme. Buildings and climate change: Summary for decision-makers. 2009.
- Yee S, Baker J, Brand L, Wells J. Energy savings from system efficiency improvements in Iowa's HVAC save program. US. DOE. Aug, 2013.
- IEA. Technology roadmap: Energy-efficient buildings: heating and cooling equipment. 2011.
- Yu Yuebin, Liu Mingsheng, Li Haorong, Yu Daihong, Loftness Vivian. Synergization of air handling units for high energy efficiency in office buildings: Implement methodology and performance evaluation. *Energy Build* 2012;54: 426–35.
- Song Zhen, Loftness Vivian, Ji Kun, Zheng Sam, Lasternas Bertrand, Marion Flore, et al. Advanced integrated control for building operations to achieve 40% energy savings. US DOE, Final report: DE-EE0003843. 2012. <http://www.osti.gov/scitech/servlets/purl/1059657>
- Yao Ye, Chen Jing. Global optimization of a central air-conditioning system using decomposition–coordination method. *Energy Build* 2010;42(5): 570–83.
- Yu Yuebin, Loftness Vivian, Yu Daihong. Multi-structural fast nonlinear model-based predictive control of a hydronic heating system. *Build Environ* 2013;69:131–48.
- Niu Fuxin, Yu Yuebin, Yu Daihong, Li Haorong. Heat and mass transfer performance analysis and cooling capacity prediction of earth to air heat exchanger. *Appl Energy* 2015;137:211–21.
- Lior Noam. Sustainable energy development: the present situation and possible paths to the future. *Energy* 2012;35(10): 3976–94.
- Xu Xinhua, Wang Shengwei, Wang Jinbo, Xiao Fu. Active pipe-embedded structures in buildings for utilizing low-grade energy sources: a review. *Energy Build* 2010;42:1567–81.
- Yu Yuebin, Li Haorong, Niu Fuxin, Yu Daihong. Investigation of a coupled geothermal cooling system with earth tube and solar chimney. *Appl Energy* 2014;114:209–17.
- Yang CM, Chen CC, Chen SL. Energy-efficient air conditioning system with combination of radiant cooling and periodic total heat exchanger. *Energy* 2013;59:467–77.
- Vangtook P, Chirarattananon S. Application of radiant cooling as a passive cooling option in hot humid climate. *Build Environ* 2007;42(2):543–56.
- Hu R, Niu JL. A review of the application of radiant cooling & heating systems in Mainland China. *Energy Build* 2012;52:11–9.
- Stetiu C. Energy and peak power savings potential of radiant cooling systems in US commercial buildings. *Energy Build* 1999;30:127–38.

- 20 Zhang DL, Cai N, Wang ZJ. Experimental and numerical analysis of lightweight radiant floor heating system. *Energy Build* 2013;61:260–6.
- 21 Mazo J, Delgado M, Marin JM, Zalba B. Modeling a radiant floor system with phase change material (PCM) integrated into a building simulation tool: Analysis of a case study of a floor heating system coupled to a heat pump. *Energy Build* 2012;47:458–66.
- 22 Karabay H, Arıcı M, Sandık M. A numerical investigation of fluid flow and heat transfer inside a room for floor heating and wall heating systems. *Energy Build* 2013;67:471–8.
- 23 Mikeska T, Svendsen S. Study of thermal performance of capillary micro tubes integrated into the building sandwich element made of high performance concrete. *Appl Therm Eng* 2013;52:576–84.
- 24 Olesen Bjarne. Radiant floor cooling systems. *ASHRAE J Sep.* 2008:16–22.
- 25 Krzaczek M, Kowalczyk Z. Thermal barrier as a technique of indirect heating and cooling for residential buildings. *Energy Build* 2011;43:823–37.
- 26 De Paepe M, Janssens A. Thermo-hydraulic design of earth-air heat exchangers. *Energy Build* 2003;35(4):389–97.
- 27 Yang Zhenyu, Pedersen Gerulf KM, Larsen Lars FS, Thybo Hongliang. Modeling and control of indoor climate using a heat pump based floor heating system. In: *Proceedings of the 33rd Annual Conference of the IEEE Industrial Electronics Society*; 2007. p. 574–9. Taipei, Taiwan.
- 28 Kontoleon KJ, Bikas DK. The effect of south wall's outdoor absorption coefficient on time lag, decrement factor and temperature variations. *Energy Build* 2007;39:1011–8.